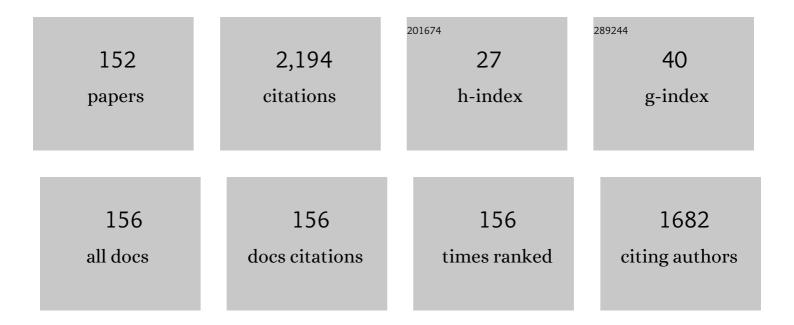
## Francesco G Della Corte

List of Publications by Year in descending order

Source: https://exaly.com/author-pdf/3548142/publications.pdf Version: 2024-02-01



#	Article	IF	CITATIONS
1	Temperature dependence of the thermo-optic coefficient in crystalline silicon between room temperature and 550 K at the wavelength of 1523 nm. Applied Physics Letters, 1999, 74, 3338-3340.	3.3	179
2	Temperature dependence of the thermo-optic coefficient of InP, GaAs, and SiC from room temperature to 600 K at the wavelength of 1.5 μm. Applied Physics Letters, 2000, 77, 1614-1616.	3.3	109
3	Temperature dependence analysis of the thermo-optic effect in silicon by single and double oscillator models. Journal of Applied Physics, 2000, 88, 7115-7119.	2.5	89
4	High-Performance Temperature Sensor Based on 4H-SiC Schottky Diodes. IEEE Electron Device Letters, 2015, 36, 720-722.	3.9	69
5	Amorphous silicon waveguides and light modulators for integrated photonics realized by low-temperature plasma-enhanced chemical-vapor deposition. Optics Letters, 1996, 21, 2002.	3.3	65
6	Temperature dependence of the thermo-optic coefficient of lithium niobate, from 300 to 515 K in the visible and infrared regions. Journal of Applied Physics, 2005, 98, 036101.	2.5	64
7	DESIGN CONSIDERATIONS FOR RADIO FREQUENCY ENERGY HARVESTING DEVICES. Progress in Electromagnetics Research B, 2012, 45, 19-35.	1.0	53
8	An Indoor Ultrasonic System for Autonomous 3-D Positioning. IEEE Transactions on Instrumentation and Measurement, 2019, 68, 2507-2518.	4.7	53
9	4H-SiC p-i-n diode as Highly Linear Temperature Sensor. IEEE Transactions on Electron Devices, 2016, 63, 414-418.	3.0	47
10	Study of the thermo-optic effect in hydrogenated amorphous silicon and hydrogenated amorphous silicon carbide between 300 and 500 K at 1.55 μm. Applied Physics Letters, 2001, 79, 168-170.	3.3	43
11	An Analytical Model of the Forward I– V Characteristics of 4H-SiC p-i-n Diodes Valid for a Wide Range of Temperature and Current. IEEE Transactions on Power Electronics, 2011, 26, 2835-2843.	7.9	42
12	85–440 K Temperature Sensor Based on a 4H-SiC Schottky Diode. IEEE Sensors Journal, 2016, 16, 6537-6542.	4.7	40
13	Thermo-optic effect exploitation in silicon microstructures. Sensors and Actuators A: Physical, 1998, 71, 19-26.	4.1	39
14	Ranging RFID Tags With Ultrasound. IEEE Sensors Journal, 2018, 18, 2967-2975.	4.7	38
15	Analysis of Trapping Effects on the Forward Current–Voltage Characteristics of Al-Implanted 4H-SiC p-i-n Diodes. IEEE Transactions on Electron Devices, 2018, 65, 3371-3378.	3.0	37
16	Use of Amorphous Silicon for Active Photonic Devices. IEEE Transactions on Electron Devices, 2013, 60, 1495-1505.	3.0	36
17	A Microsystem Based on Porous Silicon-Glass Anodic Bonding for Gas and Liquid Optical Sensing. Sensors, 2006, 6, 680-687.	3.8	35
18	Numerical Simulation Study of a Low Breakdown Voltage 4H-SiC MOSFET for Photovoltaic Module-Level Applications. IEEE Transactions on Electron Devices, 2018, 65, 3352-3360.	3.0	34

#	Article	IF	CITATIONS
19	Electro-optical modulation at 1550 nm in an as-deposited hydrogenated amorphous silicon p-i-n waveguiding device. Optics Express, 2011, 19, 2941.	3.4	33
20	Electro-optically induced absorption in α-Si:H/α-SiCN waveguiding multistacks. Optics Express, 2008, 16, 7540.	3.4	32
21	Numerical simulations of the electrical transport characteristics of a Pt/n-GaN Schottky diode. Japanese Journal of Applied Physics, 2017, 56, 094301.	1.5	30
22	Multiobjective Optimization of Design of 4H-SiC Power MOSFETs for Specific Applications. Journal of Electronic Materials, 2019, 48, 3871-3880.	2.2	30
23	Temperature and SiO2/4H-SiC interface trap effects on the electrical characteristics of low breakdown voltage MOSFETs. Applied Physics A: Materials Science and Processing, 2019, 125, 1.	2.3	30
24	A Real-Time Decision Platform for the Management of Structures and Infrastructures. Electronics (Switzerland), 2019, 8, 1180.	3.1	30
25	Simulation and analysis of the current–voltage–temperature characteristics of Al/Ti/4H-SiC Schottky barrier diodes. Japanese Journal of Applied Physics, 2019, 58, 014002.	1.5	29
26	Analysis of the Forward I–V Characteristics of Al-Implanted 4H-SiC p-i-n Diodes with Modeling of Recombination and Trapping Effects Due to Intrinsic and Doping-Induced Defect States. Journal of Electronic Materials, 2018, 47, 1414-1420.	2.2	29
27	Highly Linear Temperature Sensor Based on 4H-Silicon Carbide p-i-n Diodes. IEEE Electron Device Letters, 2015, 36, 1205-1208.	3.9	28
28	Mobile Synchronization Recovery for Ultrasonic Indoor Positioning. Sensors, 2020, 20, 702.	3.8	28
29	New possibilities for efficient silicon integrated electro-optical modulators. Optics Communications, 1991, 86, 228-235.	2.1	27
30	Simple and Low-Cost Photovoltaic Module Emulator. Electronics (Switzerland), 2019, 8, 1445.	3.1	26
31	Simulation and experimental results on the forward J–V characteristic of Al implanted 4H–SiC p–i–n diodes. Microelectronics Journal, 2007, 38, 1273-1279.	2.0	25
32	An Analytical Model of the Switching Behavior of 4H-SiC p\$^{m +}\$ -n-n\$^{m +}\$ Diodes from Arbitrary Injection Conditions. IEEE Transactions on Power Electronics, 2012, 27, 1641-1652.	7.9	25
33	Experimental characterization and numerical analysis of the 4H-SiC p–i–n diodes static and transient behaviour. Microelectronics Journal, 2008, 39, 1594-1599.	2.0	23
34	A 25 ns switching time MachÂZehnder modulator in as-deposited a-Si:H. Optics Express, 2012, 20, 9351.	3.4	22
35	Temperature Effects on the Efficiency of Dickson Charge Pumps for Radio Frequency Energy Harvesting. IEEE Access, 2018, 6, 65729-65736.	4.2	20
36	Numerical Simulations of a 4H-SiC BMFET Power Transistor with Normally-Off Characteristics. Materials Science Forum, 0, 679-680, 621-624.	0.3	19

#	Article	IF	CITATIONS
37	Instrumented infrastructures for damage detection and management. , 2017, , .		19
38	Open-Source Hardware Platforms for Smart Converters with Cloud Connectivity. Electronics (Switzerland), 2019, 8, 367.	3.1	19
39	Dynamic impedance matching network for RF energy harvesting systems. , 2014, , .		18
40	SPICE modelling of a complete photovoltaic system including modules, energy storage elements and a multilevel inverter. Solar Energy, 2014, 107, 338-350.	6.1	18
41	A Monolithic Multisensor Microchip with Complete On-Chip RF Front-End. Sensors, 2018, 18, 110.	3.8	18
42	An integrated pressure-driven microsystem based on porous silicon for optical monitoring of gaseous and liquid substances. Physica Status Solidi (A) Applications and Materials Science, 2007, 204, 1459-1463.	1.8	17
43	Analytical Modeling of Dual-Junction Tandem Solar Cells Based on an InGaP/GaAs Heterojunction Stacked on a Ge Substrate. Journal of Electronic Materials, 2019, 48, 4107-4116.	2.2	17
44	Electrooptical Modulating Device Based on a CMOS-Compatible <formula formulatype="inline"> <tex notation="TeX">\${m alpha}\$</tex> </formula> -Si:H/ <formula formulatype="inline"&gt; <tex notation="TeX">\${m alpha}\$</tex> -SiCN Multistack Waveguide. IEEE Journal of Selected Topics in Quantum Electronics, 2010, 16, 173-178.</formula 	2.9	16
45	V <sub>2</sub> O <sub>5</sub> /4H-SiC Schottky Diode Temperature Sensor: Experiments and Model. IEEE Transactions on Electron Devices, 2018, 65, 687-694.	3.0	15
46	Simulating Signal Aberration and Ranging Error for Ultrasonic Indoor Positioning. Sensors, 2020, 20, 3548.	3.8	15
47	Battery-less smart RFID tag with sensor capabilities. , 2012, , .		14
48	CMOS RF Transmitters with On-Chip Antenna for Passive RFID and IoT Nodes. Electronics (Switzerland), 2019, 8, 1448.	3.1	14
49	Performance assessment of an enhanced RFID sensor tag for long-run sensing applications. , 2014, , .		13
50	Integrated Amorphous Silicon p-i-n Temperature Sensor for CMOS Photonics. Sensors, 2016, 16, 67.	3.8	13
51	Energy savings in transportation: Setting up an innovative SHM method. Mathematical Modelling of Engineering Problems, 2018, 5, 323-330.	0.5	13
52	A parametric study of laser induced ablation–oxidation on porous silicon surfaces. Journal of Physics Condensed Matter, 2008, 20, 265009.	1.8	12
53	Low-loss amorphous silicon waveguides grown by PECVD on indium tin oxide. Journal of the European Optical Society-Rapid Publications, 0, 5, .	1.9	12
54	Temperature Sensing Characteristics and Long Term Stability of Power LEDs Used for Voltage vs. Junction Temperature Measurements and Related Procedure. IEEE Access, 2020, 8, 43057-43066.	4.2	12

#	Article	IF	CITATIONS
55	CMOS wireless temperature sensor with integrated radiating element. Sensors and Actuators A: Physical, 2010, 158, 169-175.	4.1	11
56	All-optical modulation in a CMOS-compatible amorphous silicon-based device. Journal of the European Optical Society-Rapid Publications, 0, 7, .	1.9	11
57	An autonomous and energy efficient Smart Sensor Platform. , 2014, , .		11
58	A V2O5/4H-SiC Schottky diode-based PTAT sensor operating in a wide range of bias currents. Sensors and Actuators A: Physical, 2018, 269, 171-174.	4.1	11
59	<pre><inline-formula><math display="inline" overflow="scroll"><mn>1</mn><mo></mo><mn>5</mn><mn>5</mn><mo>-</mo><mi>μ&lt;</mi><mstyle mathvariant="normal"><mtext>m</mtext></mstyle></math></inline-formula> silicon-based reflection-type waveguide-integrated thermo-optic switch. Optical Engineering, 2003, 42, 2835.</pre>	1.0	10
60	Analysis of the Electrical Characteristics of Mo/4H-SiC Schottky Barrier Diodes for Temperature-Sensing Applications. Journal of Electronic Materials, 2020, 49, 1322-1329.	2.2	10
61	In-guide pump and probe characterization of photoinduced absorption in hydrogenated amorphous silicon thin films. Journal of Applied Physics, 2006, 100, 033104.	2.5	9
62	Design and modeling of a novel 4H-SiC normally-off BMFET transistor for power applications. , 2010, , .		8
63	Amorphous silicon waveguides grown by PECVD on an Indium Tin Oxide buried contact. Optics Communications, 2012, 285, 3088-3092.	2.1	8
64	Hydrogenated amorphous silicon multi-SOI waveguide modulator with low voltage–length product. Optics and Laser Technology, 2013, 45, 204-208.	4.6	8
65	Electro-optical effect in hydrogenated amorphous silicon-based waveguide-integrated p-i-p and p-i-n configurations. Optical Engineering, 2013, 52, 087110.	1.0	8
66	Using ANT Communications for Node Synchronization and Timing in a Wireless Ultrasonic Ranging System. , 2017, 1, 1-4.		8
67	Interface Trap Effects in the Design of a 4H-SiC MOSFET for Low Voltage Applications. , 2018, , .		8
68	An Efficient 4H-SiC Photodiode for UV Sensing Applications. Electronics (Switzerland), 2021, 10, 2517.	3.1	8
69	Analytical model for the forward current of Al implanted 4H-SiC p-i-n diodes in a wide range of temperatures. , 2009, , .		7
70	A self-consistent model of the static and switching behaviour of 4H-SiC diodes. , 2010, , .		7
71	Numerical Analysis of Electro-Optical Modulators Based on the Amorphous Silicon Technology. Journal of Lightwave Technology, 2014, 32, 2399-2407.	4.6	7
72	Electro-Optical Modulation in a 4H-SiC Slab Induced by Carrier Depletion in a Schottky Diode. IEEE Photonics Technology Letters, 2018, 30, 877-880.	2.5	7

#	Article	IF	CITATIONS
73	Analysis of 4H-SiC MOSFET with distinct high-k/4H-SiC interfaces under high temperature and carrier-trapping conditions. Applied Physics A: Materials Science and Processing, 2020, 126, 1.	2.3	7
74	Enhanced Non-Uniformity Modeling of 4H-SiC Schottky Diode Characteristics Over Wide High Temperature and Forward Bias Ranges. IEEE Journal of the Electron Devices Society, 2020, 8, 1339-1344.	2.1	7
75	Simulation Study of Carbon Vacancy Trapping Effect on Low Power 4H-SiC MOSFET Performance. Silicon, 2021, 13, 3629-3637.	3.3	7
76	Electro-optically induced absorption in \$alpha\$-Si:H/\$alpha\$-SiCN waveguiding multistacks. Journal of the European Optical Society-Rapid Publications, 0, 5, .	1.9	6
77	Heat flux sensor for power loss measurements of switching devices. , 2013, , .		6
78	A calorimetry-based measurement apparatus for switching losses in high power electronic devices. , 2016, , .		6
79	Acoustic Simulation for Performance Evaluation of Ultrasonic Ranging Systems. Electronics (Switzerland), 2021, 10, 1298.	3.1	6
80	Highâ^'Performance 4Hâ^'SiC UV pâ^'iâ^'n Photodiode: Numerical Simulations and Experimental Results. Electronics (Switzerland), 2022, 11, 1839.	3.1	6
81	Photoinduced absorption in B-doped hydrogenated amorphous silicon alloys applied to all-optical modulators. Journal of Applied Physics, 2008, 103, 023107.	2.5	5
82	Steady-State Analysis of a Normally-Off 4H-SiC Trench Bipolar-Mode FET. Materials Science Forum, 2013, 740-742, 942-945.	0.3	5
83	Analysis of Al <sub>2</sub> O <sub>3</sub> high-k gate dielectric effect on the electrical characteristics of a 4H-SiC low-power MOSFET. , 2019, , .		5
84	Analysis of the current-voltage-temperature characteristics of Wl4H-SiC Schottky barrier diodes for high performance temperature sensors. , 2019, , .		5
85	LED junction temperature prediction using machine learning techniques. , 2020, , .		5
86	A Technique for Improving the Precision of the Direct Measurement of Junction Temperature in Power Light-Emitting Diodes. Sensors, 2021, 21, 3113.	3.8	5
87	Temperature dependence of the thermo-optic coefficient in 4H-SiC and GaN slabs at the wavelength of 1550Ânm. Scientific Reports, 2022, 12, 4809.	3.3	5
88	Thermo-optic design for microwave and millimeter-wave electromagnetic power microsensors. Applied Optics, 2002, 41, 3601.	2.1	4
89	Optical Interconnects for Network on Chip. , 2006, , .		4
90	An integrated hybrid optical device for sensing applications. Physica Status Solidi C: Current Topics in Solid State Physics, 2007, 4, 1946-1950.	0.8	4

#	Article	IF	CITATIONS
91	Modulation speed improvement in a Fabry–Perot thermo-optical modulator through a driving signal optimization technique. Optical Engineering, 2009, 48, 074601.	1.0	4
92	Static and transient analysis of a 4H-SiC trench Bipolar Mode FET with normally-off characteristics. , 2012, , .		4
93	Progress towards a high-performing a-Si:H-based electro-optic modulator. Journal of Optics (United) Tj ETQq1 1	0.784314 2.2	rg&T /Overloo
94	A Direct Junction Temperature Measurement Technique for Power LEDs. , 2018, , .		4
95	Power MOSFET Intrinsic Diode as a Highly Linear Junction Temperature Sensor. IEEE Sensors Journal, 2019, 19, 11034-11040.	4.7	4
96	Reconfigurable UHF RFID tag with sensing capabilities. , 2019, , .		4
97	A Technique for the Direct Measurement of the Junction Temperature in Power Light Emitting Diodes. IEEE Sensors Journal, 2021, 21, 6293-6299.	4.7	4
98	Exploiting RFID technology for Indoor Positioning. , 2021, , .		4
99	Amorphous silicon waveguides and interferometers for low-cost silicon optoelectronics. , 1998, 3278, 286.		3
100	Measurement of the IR absorption induced by visible radiation in amorphous silicon and silicon carbide thin films by an in-guide technique. Optical Materials, 2008, 30, 1240-1243.	3.6	3
101	On-Chip Integrated Antenna Structures for Biomedical Implantable Sensors. Procedia Chemistry, 2009, 1, 513-516.	0.7	3
102	HELIOS: photonics electronics functional integration on CMOS. Proceedings of SPIE, 2010, , .	0.8	3
103	CMOS fully integrated 2.5GHz active RFID tag with on-chip antenna. , 2010, , .		3
104	1.55 μm silicon-based reflection-type waveguide-integrated thermo-optic 2 × 2 switch. Optik, 2012, 123, 467-469.	2.9	3
105	Electronic sensors for intraoral force monitoring: state-of-the-art and comparison. Procedia CIRP, 2019, 79, 730-733.	1.9	3
106	Impact of a non-uniform p-base doping concentration on the electrical characteristics of a low power MOSFET in 4H-SiC. , 2019, , .		3
107	Simulation and analysis of the forward bias current–voltage–temperature characteristics of W/4H-SiC Schottky barrier diodes for temperature-sensing applications. Solid State Electronics Letters, 2020, 2, 49-54.	1.0	3
108	Study and Assessment of Defect and Trap Effects on the Current Capabilities of a 4H-SiC-Based Power MOSFET. Electronics (Switzerland), 2021, 10, 735.	3.1	3

1

#	ARTICLE	IF	CITATIONS
109	Ranging with Frequency Dependent Ultrasound Air Attenuation. Sensors, 2021, 21, 4963.	3.8	3
110	Indoor Object Positioning using Smartphone and RFID or QRCode. , 2020, , .		3
111	Performance Evaluation of Silicon and GaN Switches for a Small Wireless Power Transfer System. Energies, 2022, 15, 3029.	3.1	3
112	Silicon-on-insulator guided-wave structures for thermo-optic switching applications. , 1997, 3007, 22.		2
113	Simulation study of the DC and AC characteristics of an a-Si:H(n)/GaAs(p)/GaAs(n) heterojunction bipolar transistor. Solid-State Electronics, 2000, 44, 2265-2271.	1.4	2
114	Digital optical switch based on amorphous silicon waveguide. , 2003, , .		2
115	Li batteries with porous sol–gel cathodes. Microelectronics Journal, 2007, 38, 637-641.	2.0	2
116	A microchip integrated temperature sensor with RF communication channel and on-chip antenna. Procedia Chemistry, 2009, 1, 473-476.	0.7	2
117	Numerical simulations of Al implanted 4H-SiC diodes modeling an explicit carrier trap effect due to the non-substitutional Al doping concentration. , 2009, , .		2
118	Wireless temperature sensor integrated circuits with on-chip antennas. , 2010, , .		2
119	Autonomous RFID sensor platform with highly efficient energy harvesting circuit. , 2015, , .		2
120	A PTAT-based Heat-flux Sensor for the Measurement of Power Losses through a Calorimetric Apparatus. Procedia Engineering, 2016, 168, 1617-1620.	1.2	2
121	SPICE modelling and experiments on a complete photovoltaic system including cells, storage elements, inverter and load. , 2016, , .		2
122	Tiny Machine Learning Techniques for Driving Behavior Scoring in a Connected Car Environment. , 2021, , .		2
123	Study of in-gap defects in intrinsic and B-doped a-Si1â^'xCx:H by photo-induced optical absorption and photoluminescence. Journal of Non-Crystalline Solids, 2006, 352, 2647-2651.	3.1	1
124	Bistable hybrids in sol–gel technology for switching devices. Microelectronics Journal, 2007, 38, 1169-1174.	2.0	1
125	Electro-optical modulating multistack device based on the CMOS-compatible technology of amorphous silicon. Journal of the European Optical Society-Rapid Publications, 0, 5, .	1.9	1

Low-power CMOS fully integrated transmitters exploiting on-chip antennas. , 2010, , .

8

#	Article	IF	CITATIONS
127	Characterization of an electrically induced refractive index change in a hydrogenated amorphous silicon multistack waveguide. , 2011, , .		1
128	Design and implementation of high resolution, high linearity temperature sensor in CMOS process. , 2015, , .		1
129	RF-powered UHF-RFID analog sensors platform. , 2015, , .		1
130	RF-Powered HF-RFID Analog Sensors Platform. Lecture Notes in Electrical Engineering, 2017, , 85-91.	0.4	1
131	Effects of the Temperature on the Efficiency Degradation in Multi-stage RF Energy Harvesters. , 2019, , .		1
132	<title>Silicon thermo-optic micromodulators for low-cost low-performance fiber-in-the-loop&lt;br&gt;applications</title> ., 1997, , .		0
133	1.55- $\hat{A}$ 'm reflection-type optical waveguide switch based on thermo-optic effect. , 2003, , .		0
134	Design and simulation of an a-Si:H/GaAs HBT with improved DC and high-frequency characteristics. , 2003, , .		0
135	Digital optical switch based on amorphous silicon waveguide. , 2003, 5117, 581.		0
136	Amorphous silicon thin film for all-optical micromodulator. , 2003, , .		0
137	All-optical modulation in thin film silicon-based waveguiding structures. , 2005, , .		0
138	Fabrication of Porous Sol-Gel Cathodes for Li Batteries. , 2006, , .		0
139	Design, fabrication, and characterization of an α-Si:H/α-SiCN multistack waveguide for electro optical modulation. , 2008, , .		0
140	2.6 GHz receiver for on-chip optical networking in 65nm CMOS technology. , 2010, , .		0
141	Electro-optical modulation and photoinduced absorption effects on a CMOS-compatible α-Si:H/α-SiCN multistack waveguide. , 2010, , .		0
142	Amorphous silicon waveguides grown by PECVD on an Indium Tin Oxide buried contact. , 2010, , .		0
143	Electro-Optical Modulating Multistack Device Based on the CMOS-Compatible Technology of Amorphous Silicon. Lecture Notes in Electrical Engineering, 2011, , 285-289.	0.4	0
144	CMOS-compatible electro-optical Mach-Zehnder modulator based on the amorphous silicon technology. , 2012, , .		0

#	Article	IF	CITATIONS
145	A CMOS IC for the real-time and wireless diagnostics of high concentration solar cells. , 2015, , .		0
146	A measurement apparatus for switching losses based on an heat-flux sensor. , 2015, , .		0
147	A Calorimetry Based System for Measuring the Power Losses of Switching Power Devices. Lecture Notes in Electrical Engineering, 2018, , 111-116.	0.4	Ο
148	Augmented Information Discovery using NFC Technology within a Platform for Disaster Monitoring. , 2020, , .		0
149	Ultrasonic Ranging using Frequency Selective Attenuation. , 2021, , .		0
150	Power LED junction temperature readout circuit based on an off-the-shelf LED driver. , 2020, , .		0
151	Junction temperature measurement in optically-activated power MOSFET. Journal of Optics (United) Tj ETQq1 1 (	0.784314 2.2	rgBT /Overloo _

Near-Infrared Graphene/4H-SiC Schottky Photodetectors. , 2022, , .

0